Field-Responsive Fluid Based Multi-degree-of-Freedom Dampers for Independently Adjustable Dissipation

Aditya Suryadi Tan and Thomas Sattel

1 Introduction

Damping is a decisive factor that influences the dissipation of energy in a vibrating system. On one hand, lack of damping in a vibrating system could lead to excessive resonance or transients with a low decay rate. In such cases, adaptive damping can potentially *calm* vibrations in the fastest time possible or allow a *smooth* transition to other states. Such options are wanted e.g. to suppress earthquake excitation effects on buildings or to improve ride comfort in passenger cars. Since the vibration excitation could vary in form and magnitude, it is preferable to have a *smart* damper, whereby the damping can be adjusted based on the requirements in different conditions.

Since the 19th century, field responsive fluids, namely the electrorheological (ER) and magnetorheological (MR) fluids, attract the researchers' interest due to their unique property that serves the aforementioned requirement [11, 18]. By utilizing these fluids in damper technology, the damper becomes a *smart* system, whereby the resulted damping can be adjusted in real-time by controlling the strength of the applied field. Up to this point, more and more ER and MR-based damper concepts with various structure designs and mechanical implementations have been investigated [19]. They find successful study applications in different vibration control systems, such as vehicle suspension systems, landing gear systems [2], seismic protection for buildings [7], cable-stayed bridges [17] and advanced prosthetic systems [3]. As commercial products, MR fluid dampers have been implemented in various cars. These pure damper elements do operate only in one direction of motion and require mechanical isolation from torques and transverse forces.

A. S. Tan (✉) · T. Sattel
Technische Universität Ilmenau, Max-Planck-Ring 12, Ilmenau 98693, Germany
e-mail: aditya-suryadi.tan@tu-ilmenau.de

T. Sattel
e-mail: thomas.sattel@tu-ilmenau.de

P. Eberhard (ed.), *Calm, Smooth and Smart*, Lecture Notes in Applied and Computational Mechanics 102, https://doi.org/10.1007/978-3-031-36143-2_16

In most of the aforementioned applications, there exist a movement in more than one spatial Degree-of-Freedom (DOF). In some cases, the spatial movement and therefore the vibration could happen even in all of the six existing spatial DOFs of a rigid body, such as at the driver seat of a truck/bus [8]. For such cases, the damping is required not only in one direction but also in all of the movement directions, yet adjustable. Most commonly, several one-directional MR/ER dampers will be implemented in the vibratory system. In the worst case, at least one element in each operating DOF's axis is required [10]. By doing so, the damping can be provided and controlled in each DOF independently. Another way is to integrate several one-directional MR/ER damper elements in one damper system, so that the one damper system can operate in several spatial DOFs. Such a damper system have been applied as haptic systems, where dissipation in a form of feedback force for the user is required in more than one direction. The number of DOFs could vary from two-DOF [1], three-DOFs [9] or even four-DOFs [12], depending on the requirements. However, using this method, the higher the number of the DOF's operating axes, the bigger the total construction volume of the damper system.

In this work, ideas for new possibilities in expanding the functionality of ER/MR dampers by going beyond the conventional design are explored. The goal of this work is to find a new design of ER/MR damper to have a compact design yet higher DOFs. Appropriate design concepts are constructed and their damping performance is investigated. So far, three general possibilities are explored and investigated, namely the extension (1) by integrating several damper elements, (2) by combining known operating modes, and (3) by adding extra control elements. The damper systems including the investigation results are presented. The advantages and disadvantages for each extension method are compared, discussed, and presented as the main contribution of this work.

2 Electrorheological and Magnetorheological Fluids

ER fluids are composed of smaller micrometer-sized electrically polarizable particles suspended in an electrically insulating liquid, whereas MR fluids consist of larger micrometer-sized suspended multi-domain, magnetically soft particles [6]. Figure 1a—OFF state shows how the particles are spread in the fluid.

These particles will form a chain-like formation when a field (either in a form of electric field strength E or magnetic field strength H) is applied, in parallel to the direction of the applied field. This is illustrated in Fig. 1a—ON state, for an applied field (symbolized by the red arrows) in the vertical direction. Due to this chain-like formation, these fluids possess yield stress $\tau_0(E/H)$, which manifests itself in the shear stress τ-shear rate $\dot{\gamma}$ characteristic shown in Fig. 1b. As it can be seen in the figure, the yield stress value varies in dependence of the applied field (E/H). The

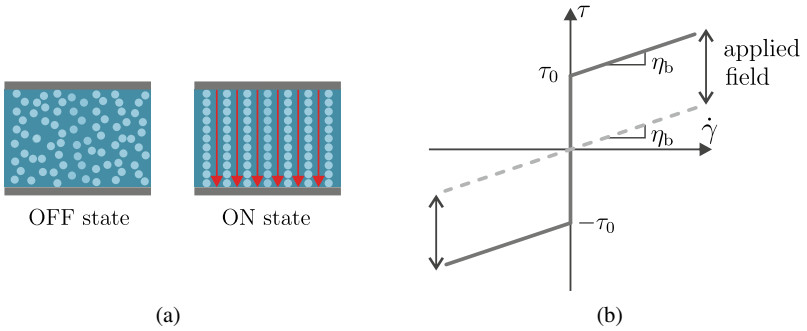

Fig. 1 **a** Principle work of field-responsive fluid and **b** its shear stress-shear rate characteristic line

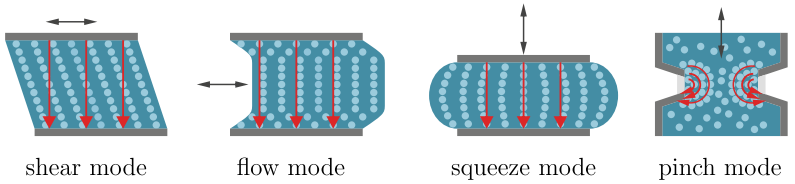

Fig. 2 Configuration of known operating modes of ER- and MR fluids

dynamic viscosity of the fluid η_b defines the gradient of the characteristic line. Due to the nature of these effects, the field-responsive material properties are restricted to the first and third quadrant of the shear stress-shear rate characteristic. The *Bingham model*

$$\tau = \begin{cases} \eta_b \dot{\gamma} + \tau_0 (E/H)\,\mathrm{sgn}(\dot{\gamma}) & \text{if} \quad |\tau| \geq \tau_0 \\ G\gamma & \text{if} \quad |\tau| < \tau_0 \end{cases} \tag{1}$$

is sufficient as the first approach to describe the qualitative behavior of the field-responsive fluid. However, there is a wide variety of existing models which allow a more precise description of these fluids, based on its operating mode [16].

The control energy which is required to operate such fluids is solely used to change their material behavior but never transferred into a transducer system. For that reason, the classification as semi-active materials is made.

Irrespective of which fluid type is employed, one of the four different working modes from Fig. 2 can be utilized. The operating and applied field direction is symbolized by the black and red arrows respectively. Depending on the operating mode, the damper will have a different design and behavior.

3 Multi Degrees-of-Freedom Field-Responsive-Fluid Based Dampers

The objective of this work is to explore the possibility of utilizing the ER/MR fluid to have a new design of a Multi DOFs (M-DOF) damper. A M-DOF damper comprises M spatial DOF in one damper element. In this work, the M-DOFs damper is realized by expanding the known conventional design of the ER/MR dampers. The extension was done by integrating several damper elements, by combining known operating modes, and by adding extra control elements, whose results are elaborated in this section.

3.1 Two DOFs ER Damper—Extension by Integrating Two Damper Elements

The simplest realization of a M-DOFs damper is by integrating several damper elements in one system. The basic idea is similar to the aforementioned systems, where several stand-alone dampers are integrated and connected into one moving body.

3.1.1 Damper Concept

For this concept, two damper elements utilizing shear operating mode are stacked together in one damper construction [13]. Figure 3a shows the operating concept of the damper.

As can be seen in this figure, the damper is a stack of two pairs of electrodes that are mounted between three parallel plates. Between each pair of the electrode plate, electrorheological fluid is contained. The bottom plate is rigidly fixed to the base and the top plate is the mounting point for a vibrating system. The electrodes are serially

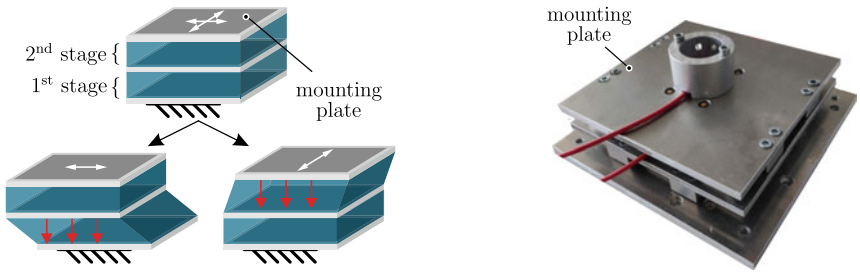

Fig. 3 **a** Principle sketch and **b** photo of the 2-DOF ER damper, uitlizing the shear mode

interconnected through two pairs of linear guides. These pairs of guides are mounted perpendicularly to each other and each pair corresponds to one pair of electrodes. Through such a mechanism, the relative motion will only occur between the two plates in which the movement direction is not constrained, which are illustrated in Fig. 3a. This concept results in a planar damper with two DOFs, whose construction is shown in Fig. 3b.

3.1.2 Operating Mode

The relative motion between two electrodes will shear the ER fluid that is placed between them, resulting in shear stress between these two plates. When this happens, the damper operates in shear mode, where the total output force of the damper can be derived from the Bingham material model in Eq. (1) together with the kinetic and kinematic relations for shear stress τ and shear rate $\dot{\gamma}$

$$\tau = \frac{F}{A_\mathrm{p}} \quad \text{and} \quad \dot{\gamma} = \frac{\dot{x}_i}{h} \,. \tag{2}$$

Here, A_p is the area of the shearing plate, $\dot{x}_i$ is the relative velocity of two moving plates in x- or y-axis and h is the gap between two plates. Inserting those relations in Eq. (1) will result in the ER-damper element model in shearing mode:

$$F_{\mathrm{d},i} = d_i\, \dot{x}_i + F_{0,i}(E_i)\, \mathrm{sgn}(\dot{x}_i) \,, \qquad i = 1, 2 \,, \tag{3}$$

$$\text{with} \quad d_i = \eta_\mathrm{b} \frac{A_{\mathrm{p},i}}{h_i} \,, \qquad F_{0,i} = \tau_{0,i}(E_i)\, A_{\mathrm{p},i} \,. \tag{4}$$

where F_d is the total damping force, d is the damping coefficients and $F_0(E)$ is the blocking forces, that are independently adjustable in each directions by variations in the electric field strengths in each stage.

In most cases, there exist a parasitic friction force that comes from both the mechanical guide and the sealing of the fluid chamber. It could be also a combination of both. These two forces will be generalized as the system friction force F_R, which can be added directly to the Eq. 3, which results in:

$$F_{\mathrm{d},i} = d_i\, \dot{x}_i + \left(F_{0,i}(E_i) + F_{\mathrm{R},i}\right)\, \mathrm{sgn}(\dot{x}_i) \quad \text{for} \quad |F_\mathrm{d}, i| \geq F_{0,i} \tag{5}$$

As it can be seen in the equation, the parasitic friction force is not dependent on the applied field but possesses the same nature as the yield force of the damper. For the case, where $|F_\mathrm{d}, i| < F_{0,i}$, there exist no velocity (the damper is assumed to have no movement).

3.1.3 Experimental Setup and Measurement Results

In this work, the ER fluid RheOil 4.0 from Fludicon is used as the damper medium. The tested damper is shown in Fig. 3b. It has a total dimension of 200 mm × 200 mm × 60 mm with an operating electrode area of 42 mm × 60 mm in each direction and a total in-plane operating range of 30 mm × 30 mm. The lower electrode pair (defined as stage 1) allows a movement along the x-axis, meanwhile the upper electrode pair (defined as stage 2) allows a movement along the y-axis. The first stage and the second stage have an electrode gap of 0.5 mm and 0.35 mm respectively. A voltage will be given at each electrode pair to vary the generated damping force.

Figure 4 shows the plots of the damping force F_d over the damper's velocity for each direction of the damper axis.

The straight line represents the force from the mathematical model in Eq. (5). The markers are the measured force obtained in the experiments. The same color is used in each plot to represent the same electric field strength. It can be seen in the plots, that the measurement results are in agreement with the mathematical model in Eq. (5). The plots show that the Bingham behavior occurs in each stage, where there exists an increase of force generated by the damper as the applied electrical field is increased. The force that exists when there is no applied electrical field (E = 0 kV/mm), is the parasitic friction force F_R that is comprised of the friction of the fluid sealing and the linear guides. It can also be seen in the plots that this friction F_R is higher for the upper stage when compared to the lower stage, which is caused by mechanical parts of the damper itself. The applied field can be increased further up to its dielectric breakdown E_db, that lies at E_db = 10 kV/mm for this fluid.

Fig. 5 displays the measurement results when the coupling of the forces between the two stages is investigated. In this experiment, the electrical field E_1 was given to the lower stage while the upper stage was moved in a prescribed manner $y(t)$. With the force F_1 in the lower stage acting orthogonally, there is no change in the upper

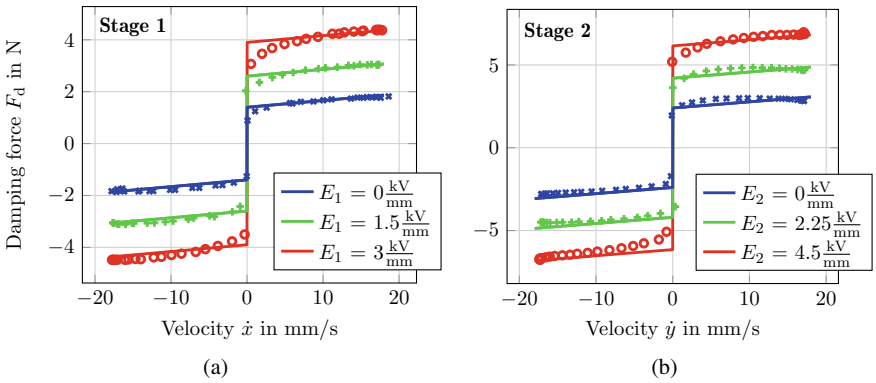

Fig. 4 Comparison between the measured (markers) and calculated (continuous lines) shear force from **a** stage 1 and **b** stage 2 for the different applied current

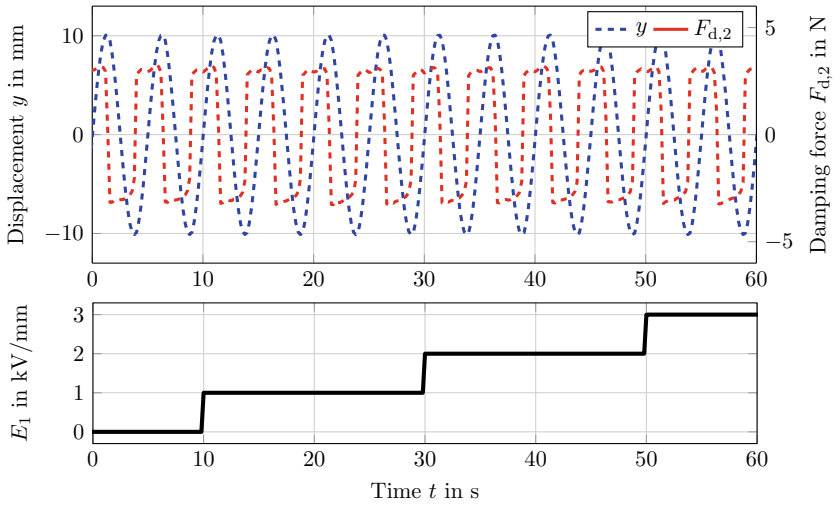

Fig. 5 Measurement result to investigate the force coupling between the stages

stage's force behavior F_2 over time. This experiment was conducted for the other stage and a similar result was obtained. The result of these experiments proved that the damping forces are independently adjustable in each orthogonal damping axis (x and y).

In conclusion, in this work, a new concept of planar electrorheological damper is introduced. This new concept of a planar electrorheological damper offers the possibility to provide two independently adjustable damping forces in two directions of movement through one integrated damping element. Moreover, the performance of such a damper was investigated and verified through experiments. The performance of the damper is shown through simulation in [13] to be promising. The difference in forces between the first and the second stage occurs due to machining tolerance. The mechanical design can be further optimized to have a larger operating range and its dimensions can be up- or downscaled easily, depending on the required damping force in the system. The main difference to the existing M-DOFs field responsive fluid-based damper is that the integration of the damper elements is done structurally, where the damper can be connected to the vibratory system at one point using one connection. Meanwhile, for the existing one, each damper element is connected to the mass individually.

The shear operating mode field responsive fluid-based damper has been proven to be useful as a tuned mass damper [14]. In comparison to a pure frictional damper, ER damper has the flexibility in adapting its yield force, resulting in a better performance. Additionally to that, due to its simple construction, where only a pair of the electrode is required to be the field source in its operation, the field can be segmented to provide another force-velocity characteristic of the damper, as proven experimentally in [15].

The main drawback of using ER fluid in comparison to the MR fluid is the low yield stress. However, the research of the giant ER fluid [5] has a prospect in covering this weakness.

3.2 Two DOFs MR Damper—Extension by Combining Operating Modes

The second extension category is combining two or more operating modes. The idea for this method is to use the operating modes that have the same mechanical configuration, yet operates in another DOF's axis.

3.2.1 Damper Concept

Possible operating modes for this method are the shear and squeeze mode of the field-responsive fluid. As it can be seen in Fig. 2, the shear and the squeeze mode have the same mechanical configuration. In both operating modes, it requires the fluid to be contained between two surfaces that have a relative motion to each other. In both modes, the field is also applied in normal direction of both surfaces. The only difference is in the axis of the relative motion. In shear mode, the relative motion is in the parallel direction to the surface, meanwhile, a relative motion in the normal direction to the surface is required in squeeze mode. Based on these points, both operating modes can be utilized by allowing the damper plate to have movement in both directions.

In order to allow the shear mode and the squeeze mode to be utilized simultaneously, the damper need to be constructed differently than common uniaxial dampers. The concept of the setup is depicted in Fig. 6a.

The idea is to have a construction, where a circular plate can be rotated in θ-direction to shear the MR-Fluid within the chamber. Thus, to allow the squeeze mode to be utilized, this rotating plate should be able to be translated in z-direction as well. This is realized by mounting the shafts using a ball bushing on each side. The circular plate is then inserted in the fluid chamber and held using two shafts, one on each side. Both the fluid chamber and the shaft are made of a non-magnetic material, presented using the yellow color in the Fig. 6. Using this configuration allows the fluid in the chamber to be sheared when the plate is rotated and to be squeezed when the plate is translated. The magnetic field is generated using the electromagnet, surrounding the fluid chamber (as shown in Fig. 6a). The surface of the iron core has the same size as the circular plate. This arrangement allows the magnetic field to be generated perpendicularly over the whole surface of the circular plate. This concept results in a two-DOFs MR damper with one fluid chamber, whose construction is shown in Fig. 6b.

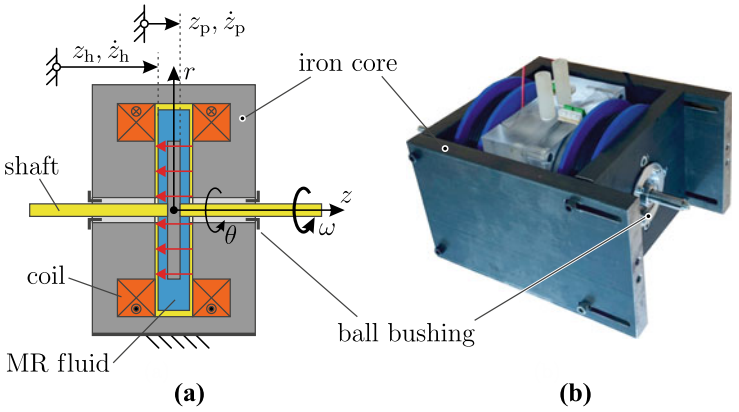

Fig. 6 **a** Principle sketch and **b** photo of the constructed 2-DOF MR damper, utilizing the shear and the squeeze mode

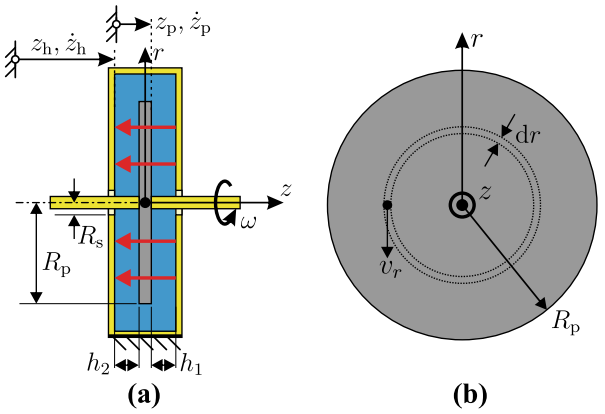

Fig. 7 **a** Cut section and **b** the surface of the 2-DOF MR damper, utilizing the shear and the squeeze mode

3.2.2 Operating Mode

The two operating modes that are utilized in this MR damper, namely the shear and the squeeze operating mode, will be derived separately in this section. Figure 7 shows the details of the damper construction.

It can be seen from this figure that the MR fluid is present on both sides of the damper's plate. Based on this reason, the shear torque and the squeeze force need to be considered from both of the damper's sides.

Shear Mode

Different from the shear mode used in the previous two-DOFs damper, in this damper, the shear mode is caused by a rotational movement. In this case, the tangential velocity

varies along the radial axis r of the plate. Therefore, the torque M_d will be the total of all infinitesimal torques $\mathrm{d}M_\mathrm{d}$ from shear stress that acts on a small area with an infinitesimal width of $\mathrm{d}r$. The infinitesimal torque $\mathrm{d}M_\mathrm{d}$ can be derived using Eq. (1) together with the kinematic relations of the tangential velocity

$$v_r = r\,\omega \quad \text{and} \quad \dot{\gamma} = \frac{v_r}{h}, \tag{6}$$

that results in:

$$\begin{aligned} \mathrm{d}M_\mathrm{d} &= r\ \mathrm{d}F(r) = r\ \tau(r)\,\mathrm{d}A(r) \\ &\overset{(1)}{=} \eta\frac{\omega r}{h} + \tau_0(H)\mathrm{sgn}(\omega))(2\pi r\mathrm{d}r)r \\ &= 2\pi\left(\frac{\eta r^3}{h}\omega + \tau_0(H)r^2\mathrm{sgn}(\omega)\right)\mathrm{d}r \end{aligned} \tag{7}$$

The shear torque on one side of the damper is the integral of the infinitesimal torque over the operating radius:

$$M_{\mathrm{d},i} = \int_{R_\mathrm{s}}^{R_\mathrm{p}} \mathrm{d}M_\mathrm{d} = \frac{\pi\eta}{2h_i}(R_\mathrm{p}^4 - R_\mathrm{s}^4)\omega + \frac{2\pi}{3}(R_\mathrm{p}^3 - R_\mathrm{s}^3)\tau_{0_i}(H_i)\mathrm{sgn}(\omega)\,\text{for}\,i \in \{1,2\}. \tag{8}$$

Since the damper plate can be translated along the z-axis, the height on both sides is not necessarily equal. The relation between the displacement z and the gap's height is:

$$h_1 = h_0 - z \quad \text{and} \quad h_2 = h_0 + z, \quad \text{with} \quad z = z_\mathrm{p} - z_\mathrm{h} \tag{9}$$

with h_0 as the initial gap size when the plate is exactly in the middle of the fluid chamber and z_p and z_h as the displacement of the damper's plate and the housing respectively. The total shearing torque

$$M_\mathrm{d} = \left(\frac{1}{h_1} + \frac{1}{h_2}\right)\pi\eta(R_\mathrm{p}^4 - R_\mathrm{s}^4)\omega + \left(\frac{4\pi}{3}(R_\mathrm{p}^3 - R_\mathrm{s}^3)\tau_0(H) + M_\mathrm{R}\right)\mathrm{sgn}(\omega). \tag{10}$$

is the sum of the torque from both sides of the plate added by the parasitic torque M_R due to friction from sealing and guides. It is to be noted that even though the plate is moving along the z-axis, the total magnetic resistance of the magnetic circuit and therefore the magnetic field strength stay unchanged ($H = H_1 = H_2$).

Squeeze Mode

The derivation of the squeeze mode follows the derivation done in [4], where the squeeze force consists of the force due to the viscosity and the rheological effect. As done in the shear mode, the squeeze force needs to be obtained by integrating the infinitesimal force over the operating radius, which comes from multiplying the pressure differences

$$p_\eta(r) = \frac{3\eta r^2}{h^3}\dot{z}, \tag{11}$$

$$p_{\tau_0}(r) = \frac{2\tau_0 r}{h}\mathrm{sgn}(\dot{z}), \tag{12}$$

where $p_\eta(r)$ and $p_{\tau_0}(r)$ are the pressure differences due to the viscous and rheological effect respectively, with the infinitesimal area $\mathrm{d}A = 2\pi r \mathrm{d}r$. Therefore, the infinitesimal forces from each part are:

$$\mathrm{d}F_\eta(r) = \frac{6\pi\eta r^3}{h^3}\dot{z}\mathrm{d}r, \tag{13}$$

$$\mathrm{d}F_{\tau_0}(r) = \frac{4\pi\tau_0 r^2}{h}\mathrm{sgn}(\dot{z})\mathrm{d}r. \tag{14}$$

The total squeeze force on one side of the damper, $F_{\mathrm{d},i} = F_{\eta,i} + F_{\tau_0,i}$,

$$F_{\mathrm{d},i} = \frac{3}{2}\frac{\pi\eta(R_p^4 - R_s^4)}{h_i^3}\dot{z} + \frac{4\pi(R_p^3 - R_s^3)\tau_0(H)}{3h_i}\mathrm{sgn}(\dot{z}) \quad \text{for } i \in \{1, 2\} \tag{15}$$

is the total of the integrated infinitesimal forces in Eqs. (13) and (14) over the operating radius. Considering the forces on both sides of the damper's plate, the total squeeze force

$$\begin{aligned} F_\mathrm{d} = \frac{3}{2}\pi\eta(R_p^4 - R_s^4)\left(\frac{1}{h_1^3} + \frac{1}{h_2^3}\right)\dot{z} \quad \ldots \\ \ldots + \left(\frac{4}{3}\pi(R_p^3 - R_s^3)\tau_0(H)\left(\frac{1}{h_1} + \frac{1}{h_2}\right) + F_\mathrm{R}\right)\mathrm{sgn}(\dot{z}) \end{aligned} \tag{16}$$

is the addition of the squeeze force on both sides of the damper added with the parasitic friction force F_R from the sealing and guides.

3.2.3 Experimental Setup and Measurement Results

The damper plate and the shaft have a radius of 45 mm and 6 mm respectively. The fluid chamber has a height of 10 mm and the damper plate has a thickness of 5 mm respectively. This way, the damper plate will have a distance to the chamber wall of 2.5 mm when it stays in the middle of the chamber. The MR fluid utilized in this damper is the AMT-DAMPRO+ from Arus MR Tech.

For the measurement of the squeeze force F_d, the rotation of the damper is blocked. This is done by fixing the shaft and moving the housing instead. The whole damper is actuated by a linear stepper motor and guided by linear guides. This way, the movement is guaranteed to be perpendicular to the damper's plate. During the movement of the damper housing, the magnetic field is varied and the force is measured.

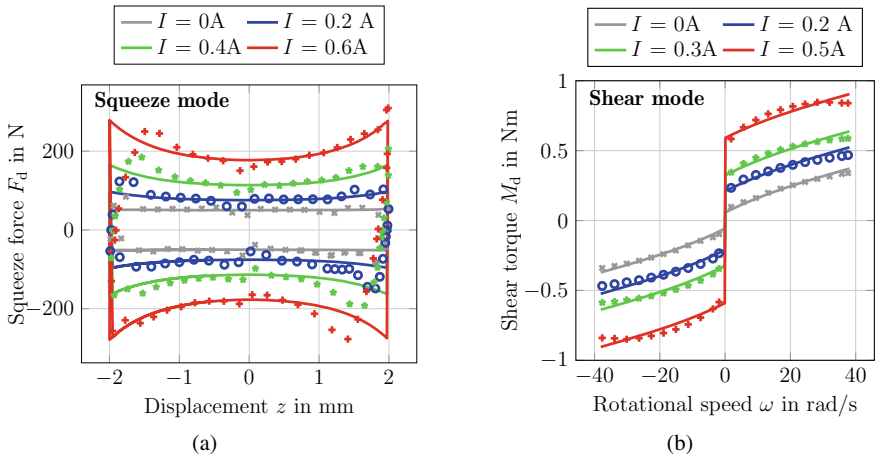

Fig. 8 Comparison between the measurement (markers) and mathematical model (continuous lines) for a **a** squeeze and **b** shear mode of the 2-DOFs MR damper

Figure 8a shows the comparison between the measured squeeze force F_d and the calculated squeeze force from Eq. (16), plotted over the displacement of the damper on the z-axis.

For the measurement of the shear torque M_d, the housing is fixed, and the shaft is rotated by a DC motor. The damper plate is initialized to be in the center of the fluid chamber so that the distance to both walls is equal ($h_1 = h_2$). Both speed rotation and the magnetic field are varied resulting in the plot in Fig. 8b, where the measured torque is compared to the one from the mathematical model in Eq. (10). For both operating modes, the measured force and torque agree with the ones from the mathematical model. In the squeeze mode, the force is increasing as the magnetic field is increased and as the damper gets close to one of the fluid's chamber walls. Thus, the plastic Bingham model in Eq. (1) only able to qualitatively model the squeeze behavior and can not perfectly represent the forces due to the dynamic effect that exists in the second and fourth quadrant of the plot. In the shear mode, the torque is increased as the magnetic field and the rotation speed is increased. In both operating modes, either from the measurement or from the mathematical model, the behavior of the Bingham fluid has been shown.

In comparison to the two-DOFs damper in Sect. 3.1, both operating modes are not completely decoupled from one another. This is the consequence of using the same fluid chamber for multiple operating modes. Therefore, the behavior of the MR damper when the damper is operated using both modes simultaneously is investigated. The investigation is done by rotating the shaft and moving the damper housing along the z-axis together. The rotational speed, the translational speed, and the magnetic field are varied during the whole process. The investigation results are presented in Fig. 9

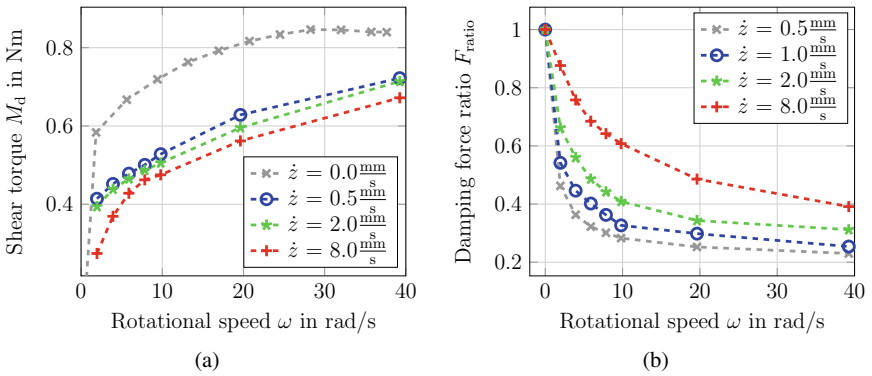

Fig. 9 Measurement results on the coupling between the operating modes

Figure 9a shows the investigation results on how the squeeze force is changed when the damper plate rotates. For that, a reference force is taken for the squeeze force when the damper's plate is at the middle position ($z = 0$). The force ratio

$$F_{\text{ratio}} = \frac{F_{\text{d},z=0}(\omega)}{F_{\text{d},z=0}(\omega = 0)} \tag{17}$$

is defined to be the ratio between the squeeze force when the damper plate is rotated and when the damper's plate is not rotated at position $z = 0$. As it can be seen in the plot, the squeeze force is decreased when a rotation exists. The faster the rotational speed the bigger is the squeeze force decreased. However, the decrement is also dependent on the squeezing speed, where the decrement is larger when the squeezing movement is slower. The same happens to the shearing torque in Fig. 9b. The shearing torque M_d is smaller when the damper plate is translated along the z-axis at the same time. For the shearing torque, the faster the squeezing speed, the bigger is the reduction of the torque.

It can be concluded, that the two-DOFs damper using this extension approach could result in a compact setup, where the same damper arrangement can be used for more DOFs. The only thing required for this improvement is the ball bushing, a mounting that allows the movement of the damper's plate exist in two directions. The damping can be adjusted in both DOFs axes. However, there exists a coupling between both operating modes, and the application of a magnetic field will affect both operating modes at the same time.

3.3 *Three DOFs MR Damper—Extension by Adding Control Elements*

The last extension category of this work is the extension by adding several control elements. In conventional ER/MR dampers, one control element is used as the field source. Since this single control element is designed to generate a field in only one direction at one certain spot, the conventional ER/MR dampers will only operate in one direction. By adding several control elements in more than one spot, the field and therefore the damping can be generated in more than one DOF axes, not only individually but also collectively.

3.3.1 Damper Concept

The suggested damper concept is with MR-Fluids, with the electromagnet as its control element. Figures 10 and 11 depict the principle sketches and the construction proposed for a three-DOF MR damper.

As it can be seen in this figure, the damper has a shape of a box. At the damper wall, four electromagnets are installed at the four sides of the damper, one electromagnet on each side, except the top and the bottom sides, see Fig. 11. A symbol of an orange triangle with the rotation degree within is given to indicate that the electromagnet's display is actually rotated in the principle sketch by 90° in comparison to the constructed MR damper for understanding purpose, where only the orientation of the electromagnet mounting is changed. The bottom side is used as the mount of the damper and the top side is used as an access for the damper to be connected with a moving system. Each electromagnet is driven by an independent power supply so that the electromagnets can be activated and therefore the magnetic field can be applied individually on the four sides of the box.

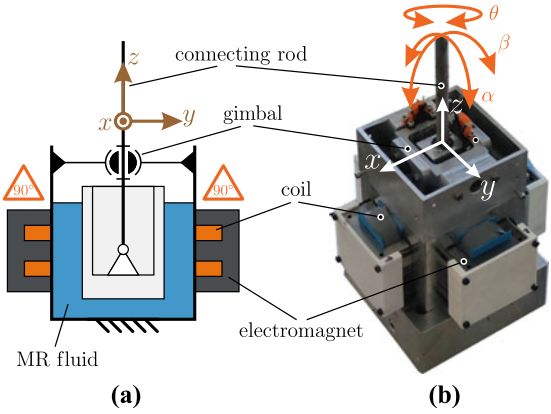

Fig. 10 **a** Principle sketch and **b** photo of the compact 3-DOF MR damper

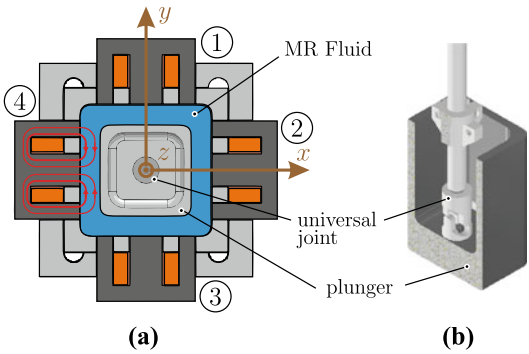

Fig. 11 **a** 2D- and **b** 3D cut section of the damper to show the joint connection

The box itself is the fluid chamber, where the MR fluid is contained. Figure 11 shows the cut section of the box in the xy-plane.

The damper plunger in Fig. 11 can be moved in any direction on the xy-plane, causing the MR fluid to be squeezed in different directions. The state of the squeezed MR fluid in a specific region can be altered by activating the corresponding electromagnet, that is attached to each side of the fluid chamber. As an example, the electromagnet 4 in Fig. 11 is activated, generating a magnetic field only on the left side of the plunger. This solidifies the MR Fluid locally in the region where the magnetic field exists and therefore increases both the flow resistance of the MR fluid in this area and the movement resistance of the plunger in this direction. Additional to that, the plunger is 3D-printed and made of a non-magnetic material. This eliminates the attraction force from the magnet to the plunger. With this configuration, the generated force is a pure damping force from the squeezed MR fluid in the respective movement direction. In Fig. 11b, there is another cut section that shows that the plunger is connected to a rod via a universal joint. This joint allows the plunger surface to be parallel to the wall of the fluid chamber when the plunger is moved by the connecting rod.

3.3.2 Operating Mode

In the previous section, it is mentioned that the MR fluid will be squeezed by the plunger. Therefore, the most suitable operating mode for this damper will be the squeeze operating mode. However, the one used in this damper is not the conventional squeeze operating mode. Figure 12 depicts the configuration comparison between the conventional squeeze mode and the one used in this work.

For this comparison, the fluid is squeezed in the vertical direction (z-axis). As it is shown in Fig. 12a, conventional squeeze mode has a magnetic field applied perpendicular to the flow direction of the fluid and to the squeezing surface. In this work, the field is not always perpendicular to the flow direction of the fluid and to the squeezing surface. As it is shown in Fig. 12b and has been proven by FEM

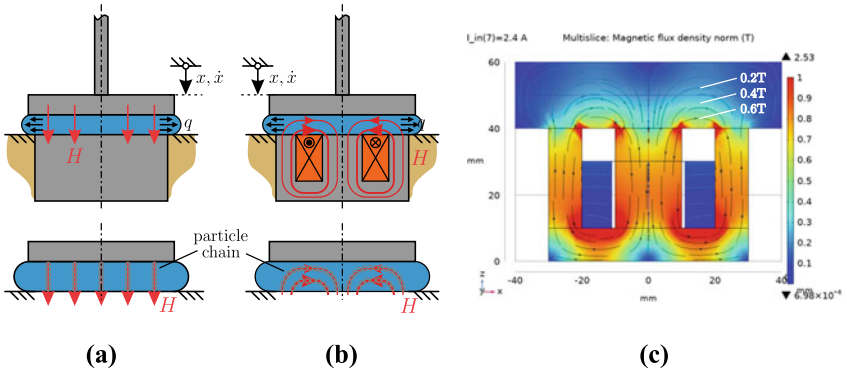

Fig. 12 Configuration comparison between **a** the conventional squeeze mode and **b** the one used for the proposed damper in this work, including **c** the FEM-analysis using COMSOL Multiphysics to investigate the magnetic field range

analysis in Fig. 12c, the magnetic field has a form of an arc. Therefore, for a different location in the fluid chamber, the magnetic field has a different vector. The difference in the magnetic field lines of both configurations made the chain-like structure of the MR fluid to have a different orientation. As it is depicted in the Fig. 12a and b, the conventional one has a chain-like structure in the form of a pillar. Meanwhile, the one with an arc magnetic field will have a chain-like structure in the form of a bridge. Based on that reason, the squeeze mode equation in the literature can not be directly implemented for this setup. This made mathematical modeling difficult and a numerical model is recommended.

However, to give an insight on how is the squeeze force in this configuration, the squeeze force will be compared to the conventional squeeze operating mode. The comparison was done by assuming that the squeezing surface in the conventional one has a radius of

$$l_\mathrm{m} = l_\mathrm{s} \frac{(1+\sqrt{2})}{4}. \tag{18}$$

where l_s is the side length of the quadratic surface of the plate and l_m is the average length between the shortest and the longest distance from the middle point to the surface edges, which are $l_\mathrm{s,short} = \frac{l_\mathrm{s}}{2}$ and $l_\mathrm{s,long} = \frac{l_\mathrm{s}}{2}\sqrt{2}$ respectively. Using the same derivation steps, as done in Sect. 3.2.2, the squeeze force

$$F_\mathrm{d} = \int_0^{l_\mathrm{m}} \left(\frac{6\pi\eta r^3}{h^3}\dot{x} + \frac{4\pi\tau_0 r^2}{h}\mathrm{sgn}(\dot{x}) \right) \mathrm{d}r \tag{19}$$

$$F_\mathrm{d} = \frac{3}{2}\frac{\pi\eta l_\mathrm{m}^4}{h^3}\dot{x} + \frac{4\pi l_\mathrm{m}^3\tau_0}{3h}\mathrm{sgn}(\dot{x}) \tag{20}$$

is the integration of the infinitesimal force $\mathrm{d}F_\mathrm{d}$, with l_m as the boundary. The calculated conventional squeeze force is then compared with the measured squeeze force

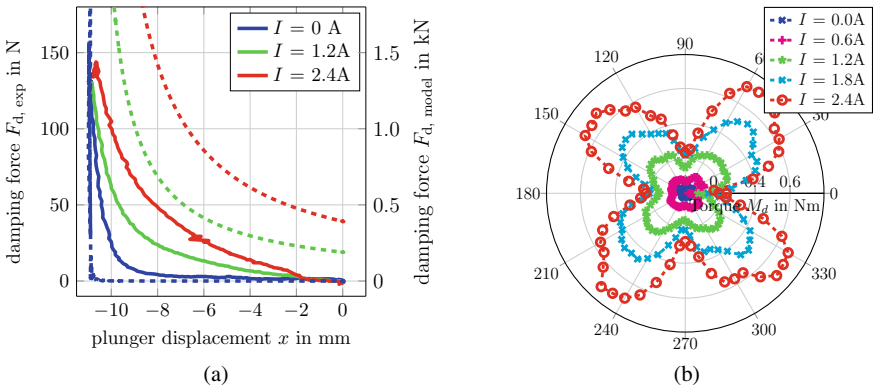

Fig. 13 **a** comparison between the calculated force for conventional squeeze mode (dashed lines) and measured force for the new squeeze mode (straight lines). **b** the measured torque for various applied field

from the new configuration (Fig. 12b), whose comparison will be presented in the next sub-section.

3.3.3 Experimental Setup and Measurement Results

The fluid chamber has a quadratic surface in this plane with a dimension of 78 mm $\times$ 78 mm. In the middle of the fluid chamber, a damper plunger with a 56 mm $\times$ 56 mm quadratic surface in xy-plane is inserted. This means that each side of the plunger has an equal distance to the wall of 11 mm. The height of the fluid chamber and the plunger can be any length, as long as it is enough to contain the fluid in the chamber during its operation. The fluid chamber is filled with magnetorheological fluid AMT-SMARTEC^{+} from Arus MR Tech.

For the first investigation, the damper behavior will be analyzed in each DOF. Figure 13 presents the results of the experiments.

Figure 13a presents the measured squeeze force when the plunger is pushed along the x or y-axis. For this investigation, only one control element is activated; the one on the side of the squeezed fluid. For the same displacement, the applied field is varied. As it can be seen in the result, the force is increased as the magnetic field is increased and as the distance between the plunger and the wall is decreased. This reflects the behavior of the squeeze mode. As a comparison, the squeeze force from Eq. (20) is presented in the same plot using dashed lines. Even though they have similar behavior, the new configuration of the squeeze mode in this works results in a smaller squeezing force. This is due to the different orientation of the field and therefore the chain-like structure of the fluid particles that causes less flow resistance in the squeezed spot. In Fig. 13b, the measured torque about the z axis is plotted over its rotational angle. For varied applied fields, the bigger the magnetic field,

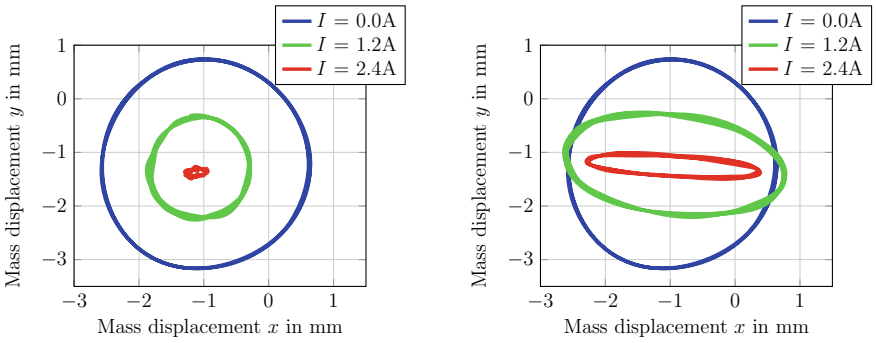

Fig. 14 Measured vibration of the damper's plunger plotted on the xy-plane

the bigger is the measured torque. Using this box configuration, the torque is not evenly distributed about the angle of rotation θ. As it can be seen in the results, the torque reach its maximum when the plunger is rotated by 45° and multiples ($\theta = \frac{\pi}{4} + n\frac{\pi}{2}$ for $\theta \in [0, 2\pi]$ with $n = 0, \ldots, 3$). The minimum torque is reached when the plunger is rotated by 90° and multiples. This is the position where the plunger's wall is parallel to the chamber's wall. These investigations have proven, that the damping can be generated and adjusted in all three DOFs of the MR damper.

As discussed in Sect. 3.2, the usage of one fluid chamber to generate damping in more than one direction has coupled the damping from one DOF to the other DOF. However, in comparison to the previous setup, this MR damper has more than one control element that is installed in different spots of the damper. It opens the possibility to adjust the damping in each DOF separately. Figure 14 is a measurement result for investigating this aspect.

A motor with an imbalance mass is attached to the damper's connecting rod, Fig. 10, resulting in vibrations in the xy-plane. This vibrations are represented by the circular movement of the plunger in this plane in both plots. Figure 14a shows the changes of the plunger movement amplitude, when all four electromagnets are activated. As the field is increased, the damping is increased in all sides of the damper and therefore the vibration amplitude is decreased evenly in all directions. That is the reason why the radius of the circle is smaller for a higher applied current. In Fig. 14b, only one pair of the electromagnet is activated, namely the electromagnets that are installed in the y-axis. This caused the reduction of the vibration amplitude only in y-axis, where the circle becomes an oval. As the field is increased, the oval is smaller. It is also investigated that the reduction of the vibration amplitude exists in the x-axis, yet much less in comparison to the reduction on the y-axis. This shows that using this extension approaches, the damping can be adjusted to be dominant only in one DOF.

4 Conclusion and Outlook

In summary, three extension approaches for MR/ER dampers have been proposed in this work. They were done by integrating several damper elements, combining existing operating modes, and adding control elements in one damper system. The proposed dampers were built and their performance is tested via experiments. The known operating modes are verified with the known mathematical model.

It can be concluded from the results, that M-DOF MR/ER damper can be realized using these extension approaches. Using the proposed methods, there is a prospect of making the damper system to be more compact. By doing so, the damper requires only one fixing point to the vibrating mass, which results in a simpler overall construction. The proposed integration of several elements allows an independent adjustment, whereas the proposed combination of operating modes and the addition of the control elements cause a coupling exists between the damping in different DOFs. Therefore, as the drawbacks of these extensions, the system becomes more complicated as the operating modes are coupled and harder to be modeled mathematically. This might demand a more complex control to regulate the damping in each DOF. Nevertheless, the work has shown that there are still a lot of possibilities for exploring the MR/ER damper design. In the future, a better way to model the damping behavior of new operating modes and the coupling of the damping in the system is required.

Acknowledgements The authors would like to express their gratitude towards the German Research Foundation, *Deutsche Forschungsgemeinschaft* (DFG) for the financial support within the priority program SPP 1897, “Calm, Smooth, and Smart”.

References

1. Ahmadkhanlou, F., Washington, G.N., Bechtel, S.E.: Modeling and control of single and two degree of freedom magnetorheological fluid-based haptic systems for telerobotic surgery. J. Intell. Mater. Syst. Struct. **20**(10), 1171–1186 (2009)
2. Choi, Y.-T., Wereley, N.M.: Vibration control of a landing gear system featuring electrorheological/magnetorheological fluids. J. Aircraft **40**(3) (2003)
3. Ekkachai, K., Tantaworrasilp, A., Nithi-Uthai, S., Tungpimolrut, K., Nilkhamhang, I.: Variable walking speed controller of MR damper prosthetic knee using neural network predictive control. In: SICE Annual Conference (SICE) (2014)
4. Farjoud, A., Cavey, R., Ahmadian, M., Craft, M.: Magneto-rheological fluid behavior in squeeze mode. Smart Mater. Struct. **18** (2009)
5. Huang, X., Wen, W., Yang, S., Sheng, P.: Mechanisms of the giant electrorheological effect. Solid State Commun. **139**(11), 581–588 (2006)
6. Janocha, H.: Adaptronics and Smart Structures. Springer, Berlin (2007). https://doi.org/10.1007/978-3-540-71967-0.
7. Lee, S.-H., Youn, K.-J., Min, K.-W.: A decentralized response-dependent MR damper for controlling building structures excited by seismic load. J. Intell. Mater. Syst. Struct. **22**(11), 1913–1927 (2011)
8. Ning, D., Du, H., Sun, S., Li, W., Zhang, B.: An innovative two-layer multiple-DOF seat suspension for vehicle whole body vibration control. IEEE/ASME Trans. Mechatron. **23**(4), 1787–1799 (2018)

9. Nguyen, H.Q., Le, T., Nguyen, D.N., Le, T.D., Lang, T.V., Ngo, T.V.: Development of 3-DOF force feedback system using spherical arm mechanism and MR brakes In: (Chunhui) Yang, R., (ed.), International Journal of Mechanical Engineering and Robotics Research, vol. 9, No. 2 (2020)
10. Oh, J.-S., Sohn, J.W., Choi, S.-B.: Applications of magnetorheological fluid actuator to Multi-DOF systems: state-of-the-art from 2015 to 2021. Actuators **11**(2), 2022 (2015)
11. Rabinow, J.: Magnetic fluid torque and force transmitting device. U.S. Patent 2575360, 1947
12. Song, B.-K., Oh, J.-S., Choi, S.B.:Design of a new 4-DOF haptic master featuring magnetorheological fluid. Adv. Mech. Eng. **6** (2014)
13. Tan, A.S., Ross, K.H., Sattel, T.: A new concept of an electrorheological planar damper for independent damping adjustment in planar movement. In: Borgmann, H., (ed.), ACTUATOR 2018: 16th International Conference on New Actuators, pp. 350–353. VDE Verlag GmbH (2018)
14. Tan, A.S., Aramendiz, J., Ross, K.H., Sattel, T., Fidlin, A.: Comparative study between dry friction and electrorheological fluid switches for tuned vibration absorbers. J. Sound Vibrat. **460**(114874) (2019)
15. Tan, A.S., Belkner, J., Stroschke, A., Sattel, T.: Damping adjustment utilizing digital electrorheological valves with parallely segmented electrodes. Smart Mater. Struct. **28**(075013) (2019)
16. Wang, D.H., Liao, W.H.: Magnetorheological fluid dampers: a review of parametric modelling. Smart Mater. Struct. **20**(2) (2011)
17. Weber, F., Distl, H.: Amplitude and frequency independent cable damping of Sutong Bridge and Russky Bridge by magnetorheological dampers. Struct. Control. Health Monit. **22**(2), 237–254 (2014)
18. Winslow, W.M.: Method and means for translating electrical impulses into mechanical force. U. S. Patent 2417850, 1947
19. Zhu, X., Jing, X., Cheng, L.: Magnetorheological fluid dampers: a review on structure design and analysis. J. Intell. Mater. Syst. Struct. **23**(8), 839–873 (2012)